In-situ microscopy investigation of floc development during coagulation-flocculation with chemical and natural coagulants

Gustavo Santos Nunes[a], Kamila Jessie Sammarro Silva[a]; Bárbara Luíza Souza Freitas[a;] Valdinei Luís Belini[b]; Lyda Patricia Sabogal-Paz[a*]

[a] Department of Hydraulic and Sanitation, São Carlos School of Engineering, University of São Paulo, Trabalhador São-Carlense Avenue 400, São Carlos, São Paulo, 13566-590, Brazil

[b] Department of Electrical Engineering, Universidade Federal de São Carlos, Rodovia Washington Luís, km 235. São Carlos, São Paulo, 13566-905, Brazil.

*Corresponding Author: lysaboga@sc.usp.br

Abstract: This study aimed to include *in-situ* microscopy in the analysis of floc development during coagulation-flocculation for drinking water treatment. To this end, jartest series were carried out for natural and synthetic waters using aluminium sulphate, sulphate chloride, ferric chloride, and *Opuntia* sp. as coagulants. Coagulation under optimized conditions was monitored by an *in-situ* microscope in conjunction with image analysis. Obtained results enabled some insights on the coagulation process. Images captured different stages of initial floc development, including flocs exhibiting heterogeneous, branched, and irregular surface structures. From image analysis, wide distributions of flocculated particle sizes were found for both natural (19–15834 μm) and synthetic water (19–21607 μm), suggesting the occurrence collisions by adhesion and transport between particles, thus influencing floc formation rates depending on the medium.

Average size and number of flocs, as determined by the image analysis algorithm as a function of the time, showed inverse correlation of floc growth with water clarification. The microscopic images also illustrated how different coagulants in different water sources undergo breaking through fragmentation or erosion. Our findings also highlight the importance of investigating additional aspects that involve conditions of mixing, development, breaking, regrouping, and resistance of flocs.

Keywords: *Opuntia cochenillifera;* image analysis; aggregates; floc development; floc rupture; treatability assays

1 Introduction

Chemical coagulation is one of the first processes in water treatment plants and it consists of disturbing particles by adding a reactive coagulant, usually iron or aluminium salts. In contact with water, these salts originate hydrolysed species that are adsorbed by the colloidal particles, which are then destabilized, due to changes in the ionic strength of the medium [1,2]. In flocculating tanks, destabilized particles are slowly agitated for a relatively long time to increase the probability of collision between particles [3,4].

During flocculation, two mechanisms may occur: adhesion and transport. The former refers to the possibility of effective collisions between particles due to coagulation, and the latter is related to the agitation introduced into the medium (perokinetic flocculation, orthokinetic flocculation, and fluid movement) [3,4]. With the addition of new products by coagulation, the characteristics of the particles change as they interact with each other. These changes interfere on collision frequencies and particle growth, since they are a function of the size and concentration

of the particles in the medium, as well as surface charge, roughness, shear forces, among others [5]. The performance of coagulation and flocculation on water treatment will depend on factors as in the characteristics of the water source (*e.g.*, pH, turbidity, true and apparent colour, temperature, particle sizes, dissolved organic matter), and operational factors such as coagulant dose, acidifying and alkalizing agents, and hydraulic characteristics [6].

Aluminium and ferric salts are the most used coagulants for drinking water treatment. These compounds are highly electropositive, form gelatinous compounds with positive charges, and react with negatively charged impurities, thus forming flocs. Some of the advantages of their application are their low cost and market availability, in addition to their known efficiency in removing colour and turbidity [4]. Aluminium-based coagulants have sulphate and aluminium chloride as their main representatives. The major factors that influence their performance are minimum pH of solubility, total aluminium concentration, and temperature [7,8]. Ferric coagulants are mainly represented by ferric chloride and sulphate, readily available in solid or liquid forms. However, it should be noted that there are also some disadvantages associated with chemical coagulants in general, such as the formation of by-products of coagulation, production of larger volumes of waste, presence of residual aluminium in the treated water, association with Alzheimer's disease, among other issues that raise public health concerns [9].

In this context, the use of natural coagulants is a rising option, mostly because they generate biodegradable residues that are easy to dispose of, in addition to their low associated cost [8,10]. Natural coagulants may be extracted from animals, microorganisms or plants, and act predominantly through the mechanisms of adsorption and neutralization of colloidal particle charges and formation of bridges. Their application has been considered promising in locations

where there is inefficient supply or deterioration of river water quality [9]. Besides, these products are considered easy to implement and efficient for water treatment [9].

Among the species of plants that present coagulating properties, those of the *Opuntia* genus stand out. For domestic use, they are applied in the form of powder or pastes, and, when conditions are optimized, they become a practical and low-cost solution suitable for use in developing communities [10]. However, there is still no standard scientific methodology for identifying the active principles of coagulation by plant extracts. Moreover, literature lacks information regarding the toxicology of these products, better elucidation of the coagulation mechanisms, and low dissemination of the results regarding application of these coagulants [11], which encourages further investigation.

The performance of coagulation and flocculation units, designed to destabilize and alter the size distribution of the colloidal particles, are related to the floc size [12]. Thus, changes in the shape, size, and volumetric distribution of the flocs directly influence treatment efficiency and may be dependent on the type of coagulant used [12]. It is common for studies to evaluate the efficiency of the coagulation and flocculation processes as a function of the concentration of particles in the medium and/or turbidity [13]. However, there is a need to monitor the process to assess other aspects of treatment, such as the influence of qualitative and quantitative aspects of the flocs, influencing the final quality of clarified water.

Studies addressing the characterization of flocs in mass, volume or characteristic particle dimension have raised relevant discussions about the relationship between floc characteristics and treatment efficiency [14]. Other approaches have also been undertaken, such as analysis of viscosity, shape, texture, fractal dimension, solidity, and roughness [14]. Flocs are fragile structures formed by a considerable amount of water that can easily break by invasive

interferences, *e.g*., by pumps and agitation devices [15]. Due to these limitations, it is preferable to use non-invasive techniques to study flocs formed during coagulation and flocculation processes [6].

Several techniques have been proposed in literature for structural characterization of flocs using non-invasive measurements, as reviewed by Jarvis et al. [16]. These techniques have allowed researchers to study flocs by taking photographs of the suspensions through a camera and illumination sources placed on the external side of transparent vessels containing the suspension. However, subjectivity associated with experimental settings (*e.g*., camera position, focus adjustments, illumination intensity) in conjunction with special conditions to acquire images, including darkened rooms [6] and flow cells [17], make it difficult to establish a systematic fashion for image acquisition, which may ultimately result in inconsistences when analysing different systems. Besides, camera-based floc characterization methods monitor particle suspension at short distances (0.3 – 1 cm) behind the wall of the tank [16], which means that flocs must travel to reach the imaging plane and therefore intermediate floc development stages might not be captured.

Accordingly, we propose to use an *in-situ* microscope to acquire images directly from suspensions to avoid subjectivities usually associated with experimental settings involving camera-based approaches, with the additional advantage of imaging much deeper floc suspensions. The proposed system was used to determine size distribution of flocs formed in different water matrices under optimized treatment conditions using chemical and natural coagulants.

Although it is still an incipient approach in water treatment studies, technological advances in data processing combined with *in-situ* microscopy can allow advances in monitoring

and evaluation of the characteristics of particles and agglomerates [18]. Therefore, the motivation for this study arises from the need to better describe the process of floc formation, understanding how their physical characteristics (shapes and sizes) interfere in the efficiency of water treatment. To investigate the dynamics of floc formation and breaking, we used *in-situ* microscopy in conjunction with image analysis algorithms. The proposed system allowed assessing the size of flocs formed in two water matrices (natural and synthetic) under optimized treatment conditions using chemical and natural coagulants.

2 Material and Methods

2.1 Chemical coagulants

Aluminium sulphate, ferric sulphate, and ferric chloride (Sigma Aldrich®) were applied as chemical coagulants. Dosages used in the preliminary treatability screening were: 10 to 60 mg L^{-1} for $Al_2(SO_4)_3$, 5 to 65 mg L^{-1} for $Fe_2(SO_4)_3$, and 5 to 65 mg L^{-1} for $FeCl_3$.

2.2 Natural coagulant

The natural coagulant extracted from *Opuntia cochenillifera* was obtained by samples of the cactus obtained in the municipality of São Carlos (São Paulo State, Brazil). First, after removing spines, the cladodes were washed in running water and cut into approximately one-centimetre fragments. The preparation of *O. cochenillifera* was based on Miller et al. [19] and Shilpa et al. [9]. Then, 0.5 kg of freshly prepared cladodes were placed in an oven lab at 60 °C for 24 hours. The dry material was crushed in a food processor and sieved at 300 μm. The retained material was crushed and sieved again. To avoid losing its properties, the powder was stored (<15 days) in a vacuum package and kept in the dark. Total and volatile solids were

quantified to estimate the amount of *O. cochenillifera* effectively measured in the treatability assays, according to APHA et al. [20]. The resulting powder was tested as a natural coagulant with dosages ranging from 10 to 60 mg L^{-1}.

2.3 Selection and preparation of water matrices

Treatability assays were performed using two matrices: natural and synthetic water. The natural water was collected directly from Monjolinho River (São Carlos, São Paulo, Brazil), while the synthetic water was a mixture of groundwater water (from a well in São Carlos, São Paulo, Brazil) with 0.2 g L^{-1} of kaolinite (Sigma Aldrich®) and 3.3 mg L^{-1} of humic acid (Sigma Aldrich®). Reservoirs of 500 L and 200 L were used for water storage and homogenization, respectively. The reservoirs were disinfected with sodium hypochlorite (NaClO) before the tests' beginning and capped to protect against external agents.

Physicochemical characterization of both water (Table S1) was performed according to the following parameters: temperature, pH, turbidity, apparent colour, true colour, partial alkalinity, total alkalinity, dissolved organic carbon, electrical conductivity, and zeta potential [20].

2.4 Treatability assays

Treatability tests were carried out on jartest (2 L). The definition of optimal coagulation conditions (dosage and pH of coagulation) was obtained from coagulation diagrams plotted on Microsoft® Excel software. Mixing parameters were set as recommended by Di Bernardo et al. [21], Miller et al. [19], and Souza Freitas and Sabogal-Paz [22]. The remaining values of colour and turbidity were recorded. After defining the dosage and pH of coagulation, we performed

tests to optimize the mixing conditions. For each coagulant, the best rapid mixing gradients, rapid mixing times, flocculation gradients, flocculation times, and sedimentation velocities were evaluated (Table 1). Optimal values were selected considering the lowest remaining turbidity value.

Parameters	Unit	Chemical coagulants*	Natural coagulant
Rapid mixing gradient	s^{-1}	1020; 1000; 900; 800; 580	200; 250; 335; 380; 430
Rapid mixing time	s	10; 15; 20; 30; 60	20; 30; 40; 50; 60
Flocculation gradient	s^{-1}	15; 20; 25; 30; 35	20; 25; 30; 35; 40
Flocculation time	min	25; 30; 35; 40; 45	10; 20; 30; 40; 45
Sedimentation velocity	cm min^{-1}	3.0; 2.5; 2.0; 1.5; 1.0	2.0; 1.5; 1.0; 0.5; 0.25

Table 1. Operating conditions assessed in treatability assays

* Aluminium sulphate, ferric sulphate, and ferric chloride

2.5 *In situ* microscopy

A custom-built high-resolution (~1.6 μm) *in situ* microscope was built to acquire microscopic images directly from suspensions. The instrument was inspired in the design presented by Suhr et al. [23]. Essentially, it is a brightfield microscope composed of a light source, objective lens (10×, NA = 0.25), and a digital camera (SCA1400–17 gm, Basler, Ahrensburg, Germany, CCD-size 8.98 mm × 6.71 mm, 1392 × 1040 pixels, pixel size 6.45 × 6.45 μm^2, bitmap, 8 bits). Based on the camera sensor size and used objective, the field of view of the imaging system is 0.66 × 0.88 mm^2. From an external light source, pulsed lighting was produced by a red LED (628 nm, 10,000 mcd) positioned in front of a quartz window, which

178 separates the suspension from the objective lens. The 6-mm separation between the quartz
179 window and the LED defines a virtual volume, in which the suspension flow through freely at
180 different suspension agitation speeds, depending on the conditions of each system analysed.

181 Due to the pulsed illumination, images of the objects that have gone through the virtual
182 volume were registered by the camera, processed, and analysed by an image analysis algorithm
183 developed on MATLAB. The gain, time of exposure of the camera, and pulse of illumination
184 were experimentally defined according to the medium and the coagulant, by performing visual
185 inspections of the acquired images. In conjunction with the length of the tube lens connecting the
186 objective lens and the camera, the optical magnification was fixed at 100× for all systems
187 analysed. Floc size distribution and the time evolution during the flocculation process were
188 obtained by the developed image analysis algorithm. Due to the agitation of the suspension, the
189 images of the flocs were distinct from each other. Therefore, they do not represent the
190 morphological evolution of a particular floc. During the measurements, only flocs in focus were
191 automatically selected by the algorithm for size and time-evolution analysis.

192 For the experiments, the *in-situ* microscope was positioned at 5 cm below the jars' water
193 column at the closure of the rapid mixing step.

194

195 **2.6 Image analysis**

196 An image analysis algorithm was implemented using the MATLAB Image Processing
197 Toolbox. Figure 1 shows the flowchart of the algorithm.

198

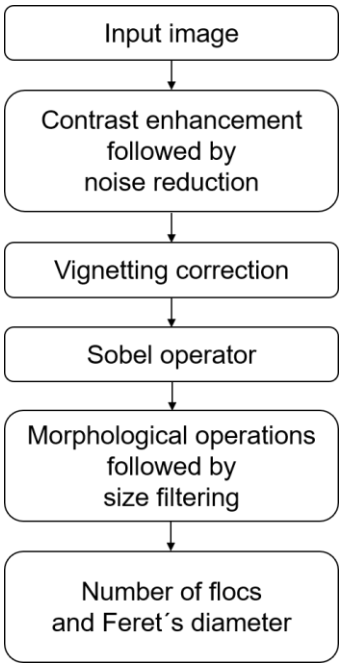

Figure 1. Flowchart of all operations of the image analysis procedure.

The first step of the procedure consisted on processing the input image to facilitate the detection of objects: the contrast of the input image was enhanced by dividing the difference between each pixel intensity in the original image by the difference between the maximum and minimum pixel intensity in that image. Subsequently, the enhanced image was smoothed by a 7 × 7 median filter to reduce high frequency noise. Due to the illumination by an LED, the ISM images suffer from some vignetting, *i.e.*, reduced brightness toward periphery compared to its center [24]. The intensity mean of the first 70 free-flocs images was used to normalize the brightness of the entire image to compensate for this effect.

To find objects in the processed image, Sobel operation was computed [25]. By using intensity threshold to the Sobel transformed images, a binary image containing closed lines of connected white pixels on a black background is created. Short gaps in the lines of pixels were closed by a morphological dilation operation [25] using 3-pixel line structuring elements.

Subsequently, opening-by-reconstruction were applied to remove small groups of connected pixels, while preserving the overall shape of the objects.

As in this step porous may still exist within objects, these were eliminated by applying the following sequence of operations: opening-closing by reconstructions, hole filling, morphological closing, and hole filling. In this step, objects larger than 500 pixels were discarded by the algorithm from further analysis because they are smaller than the expected size for flocs. Touching border objects were also removed in this step.

Once the images were processed by the above-described procedure, the number of flocs was determined as being the number of objects within each resulting image.

Finally, the Feret´s diameter was computed for each detected object. To this end, the code available in the Matlab Central File Exchange (https://www.mathworks.com/matlabcentral/fileexchange/30402-feret-diameter-and-oriented-box) was used. Each pixel corresponds to a real length given by pixel size over magnification:

$$Length\ represented\ by\ one\ pixel = \frac{6.45\ \mu m}{10} = 0.65\ \mu m \quad (1)$$

2.6 Statistical analysis

To test for a statistically significant difference in turbidity and true colour removal efficiencies considering the coagulant and water matrix types, the ANOVA and Tukey *post hoc* tests were performed in normally distributed data. Statistical analysis was carried out on Statistica 10 (TIBCO Software Inc.), and *p*-values were calculated at 5% significance level.

3 Results and Discussion

3.1 Treatability assays

Table 2 shows the efficiency of the coagulants in removing turbidity and true colour from natural and synthetic water. For natural water, Tukey's *post hoc* test indicated a significant difference ($p < 0.05$) in turbidity removal using *O. cochenillifera* when compared to aluminium sulphate and ferric sulphate. For synthetic water, Tukey test indicated a significant difference ($p < 0.05$) in the removal of turbidity using *O. cochenillifera* compared to the three chemical coagulants. Regarding true colour removal, statistical differences were observed among all coagulants for both types of water ($p < 0.05$), except for ferric coagulants treating natural water ($p > 0.05$).

As our study, Baghvand et al. [4] indicated a better performance of ferric chloride in removing turbidity compared to aluminium sulphate. Yu et al. [26] reported greater efficiency of ferric coagulants compared to aluminium ones by the hydrolysis of Fe to reach equilibrium faster than that of Al. Due to this mechanism, larger flocs can be formed by iron hydroxide precipitate formation. On the other hand, for aluminium-based coagulants, small flocs are formed slowly, affecting the coagulation performance. Similar efficiency values were found by Yang et al. [27] when evaluating the performance of aluminium sulphate; these authors observed that the surface water had 94.5% of its initial turbidity removed by the scanning mechanism, with an optimal dosage of 15 mg L^{-1} and a coagulation pH of 7.73.

Coagulant	Natural water			Synthetic water		
	Dose (mg L^{-1}); pH	Turbidity (NTU)	True colour (HU)	Dose (mg L^{-1}); pH	Turbidity (NTU)	True colour (HU)
Aluminium sulphate	20; 7.09	97.6 ± 0.5%	91.7 ± 3.6%	36; 6.36	99.5%	97.7 ± 0.5%
Ferric sulphate	22.5; 6.91	97.6 ± 0.2%	100%	30; 6.04	99.4%	99.6 ± 0.8%
Ferric chloride	15; 6.38	84.7 ± 12.7%	100%	20; 6.24	99.4 ± 0.1%	83.3 ± 1.6%
Opuntia sp.	20; 9.97	73.2 ± 0.6%	85.2 ± 0.5%	30; 9.97	97.3 ± 0.3%	20.9 ± 2.4%

Table 2. Efficiency of the coagulants used in removing turbidity and true colour from natural and synthetic water. The efficiency values are shown as mean ± standard deviation.

Our treatability results for *O. cochenillifera* indicated that, despite acting on the removal of colour and turbidity, this coagulant is not recommended without preliminary treatment, or if used, a chemical coagulant in lower dosage should be added. Miller et al. [19] tested *O. cochenillifera* for treating water with different turbidities and reported turbidity removal of up to 99%, however, remaining values ranged between 5 and 7 NTU, similar to our experiments. Shilpa et al. [9] also performed tests with *O. cochenillifera* in natural water, dosing 20 mg L^{-1} of the natural coagulant and noticed a reduction in turbidity from 83 to 9.1 NTU (89% efficiency), emphasizing the importance of maintaining the pH between 8 and 10.5.

3.2 *In-situ* microscopy analysis

3.2.1 Natural water

Figure 1 shows the time evolution of the formation of flocs through the application of different coagulants for the treatment of natural water. Images captured in seven periods of time illustrate the evolution of colloidal particles in sub-flocs and aggregates during flocculation. The images showed that the aggregate structure is a cluster of particles that form floc with irregular surface.

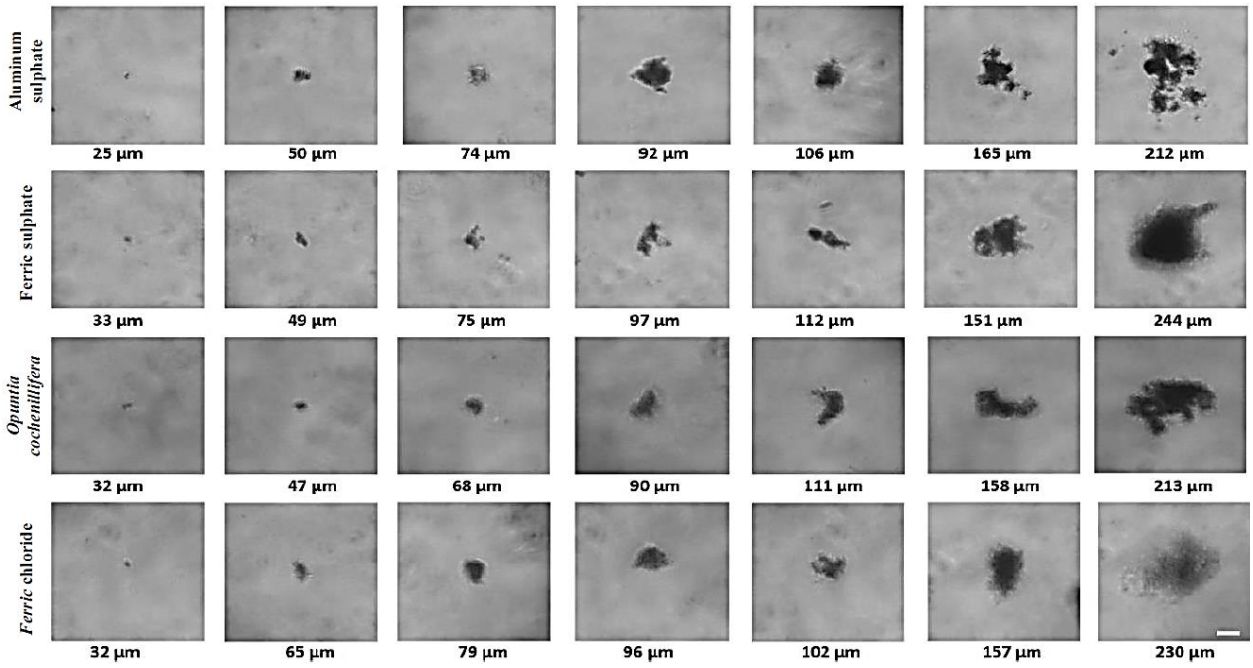

Figure 2. Examples of *in-situ* floc images captured during the natural water flocculation process using different coagulants. Non-corresponding floc portraits are shown. The portraits were cropped from original images (1392 × 1040 pixels) by the algorithm. The values indicate the Feret's diameter. The difference in sharpness is due to the turbidity and water matrix studied (Scale bar = 50 µm).

As shown, flocs can be wide, porous, branched, and irregular-shaped structures. According to Chakraborti et al. [28], the heterogeneity of floc size and shape influences aggregation and breaking rates under different physical, chemical, and hydrodynamic aspects. At the early stages of the floc formation (Figure 2), small particles (diameters ranging from 25 to 33 μm) were dispersed in the medium. Over time, these particles were covered by the precipitate and intertwined to form larger flocs of different shapes.

Turchiuli and Fargues [15] observed that floc structure was formed by three basic units: cluster (or group), aggregate, and floc *per se*. The authors found that, at the beginning of coagulation process, floc diameters achieved values between 2 and 21 μm, forming clusters. Through the agglutination process with the addition of the flocculation aid, single flocs quickly evolved to aggregates (diameter between 32 - 50 μm), which remained during flocculation. Once the process was finished and flocs began to settle, they formed aggregates up to 1160 μm in diameter, thus composing the settling sludge at the end of the primary water treatment. These authors attributed the flocs' growth with flocculation aid, as due to the high gradients of rapid mixing, so that the flocs are unable to develop dimensions larger than 21 μm.

The purpose of the rapid mix was to promote reactions between the coagulants and impurities. As in the present study images started to be captured after coagulation, what can be seen in the first records are clusters, but with dimensions greater than 21 μm. Even without the addition of flocculation aids, the aggregates reached up to 244 μm in diameter. To form flocs, these particles can also adhere to long natural polymer chains that also form flocs with heterogeneous shapes, as seen in the flocs formed using a natural coagulant (Figure 2). Due to this increase in diameter (Figure 2), a reduction in the number of particles was also observed, being an indication that particles' aggregation was occurring to form larger flocs. Moreover,

according to Lapointe and Barbeau [13], the diameter of the flocs impacts water treatment more than their density and shape. Therefore, the relative frequency of flocs of different diameters for each tested coagulant was obtained. This is displayed in Figure 3, which provides an idea of a size distribution function. Y-axis displays the relative frequency (%), and the x-axis classifies flocs formed by each coagulant in size groups based on Feret's diameter.

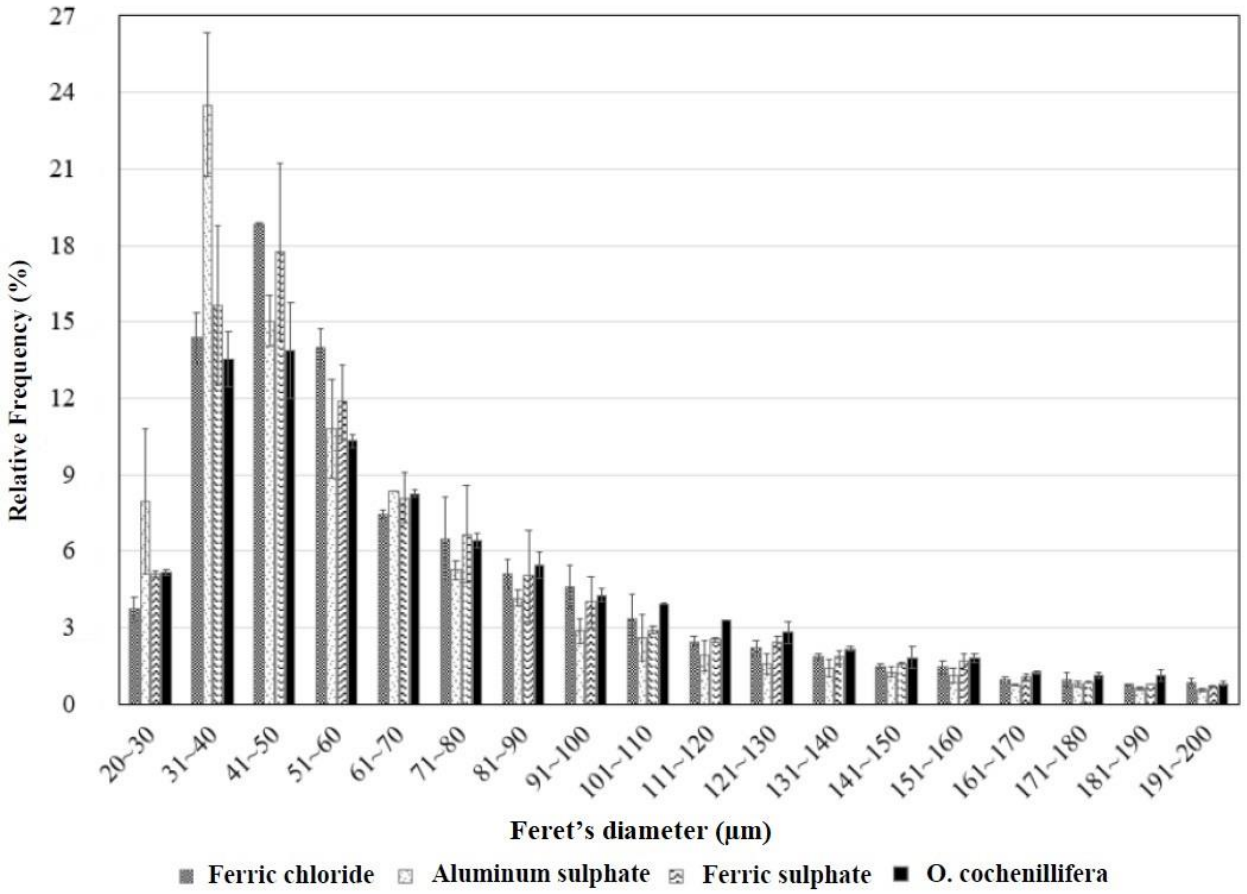

Figure 3. Relative frequency of flocs (Feret's diameter range) formed during flocculation of the natural water. The results were obtained by evaluating 500 images for each coagulant

Specifications of aggregates formed in natural water for the different coagulants are provided in the Supplementary Material (Table S2). Feret's diameter in the range 20 - 200 µm represented 90% of the diameters analysed in the natural water matrix. Considering a

conventional water treatment plant in which filtration is included, it should be noted that particles between 1 and 10 μm are challenging to be removed in filter media. That is because they can pass directly to the final stage, detach from the filter, or overload them [29]. In our study, flocs had dimensions larger than 10 μm at the beginning of the flocculation, which might contribute to longer operating times for filters in further stages of treatment. On the other hand, wide distribution in aggregate sizes (peaks between 41 and 50 μm for ferric coagulants and *O. cochenillifera* and between 31 and 40 μm for aluminium sulphate) was observed (Figure 3). Diversity of forms favours the occurrence of several collisions between aggregates, and it also influences the different rates of formation and rupture of flocs, which occur under different physical-chemical and hydrodynamic conditions. According to Turchiuli and Fargues [15], a larger number of collisions allows greater structural reorganization of the flocs and compaction of the structure as it expels water trapped internally in the structure. We noticed that diameters varied between 19 and 10839 μm (Table S2), highlighting similarities and differences between chemical and natural coagulants.

Chemical coagulants acted by the scanning mechanism and showed greater efficiency in removing colour and turbidity from natural water. According to Duan and Gregory [30], the formation of larger aggregates by the scanning mechanism occurs due to the increase of solids' concentration with the formation of precipitates. Moreover, we observed that ferric coagulants contributed to form flocs larger than the aluminium sulphate coagulant (Figure 2), similarly to the findings of Jarvis et al. [31]. Considering dissolved organic carbon (DOC), the low proportion of DOC:Fe for ferric sulphate (0.32) and ferric chloride (0.16) explains the good performance of ferric coagulants and the formation of large flocs, as studied by Jarvis et al. [16]. These authors noticed that, when the value of this ratio is high, interactions between carbon and

the floc matrix affect floc structure. On the other hand, it was expected that *O. cochenillifera*, by acting through the adsorption and bridging mechanisms, would form flocs with larger dimensions. Nevertheless, due to the flocs being larger and containing more water, the mass distribution was affected, which may have resulted in a lower sedimentation capacity and removal efficiency.

Knowing that flocs with extreme sizes end up interfering in the final values of the average diameter, we observed differences in the average size of flocs and number of flocs by analysing the generated peaks (Figure S1). The curves reached their maximum value when the diameter or the number of flocs increased sharply, while the valleys followed the peaks, where the lowest values were observed. For aluminium sulphate, the maximum mean values obtained by the flocs were 116, 122, and 133 μm, followed by minimum values 80 and 95.5 μm, similarly to Lapointe and Barbeau [13]. In addition, we observed that the largest number of flocs occurred at the beginning of the flocculation when the size of the flocs was trending towards a valley moment.

In contrast, treatment with ferric sulphate reached higher peaks than the one with aluminium sulphate, with 155 and 173.5 μm (maximum) and 90 and 93 μm (minimum), similar to findings obtained by Jarvis et al. [31]. Besides, ferric chloride assays indicated an increase in the average size of the flocs, which contributed to the formation of increasingly larger aggregates, while the decrease in the number of flocs reflected the occurrence of water clarification. On the other hand, the natural coagulant extracted from *O. cochenillifera* resulted in flocs of varying sizes and numbers. This can be explained by the concentration of organic matter in the medium and within the natural coagulant itself, providing weak associations. In applications with chemical coagulants, the organic matter involves colloidal particles preventing

366 the action of inorganic salts or forming flocs of smaller diameters [16]. These variables can
367 interfere on the operating time of slow filters, because of the low resistance of the aggregates to
368 hydrodynamic fluctuations [32].
369
370 **3.2.2 Synthetic water**
371 Figure 4 shows the temporal evolution of flocs through the application of different
372 coagulants on synthetic water. The images captured at the beginning of flocculation indicated
373 that the formation of the aggregates occurred since coagulation, once initial diameters had values
374 larger than those of kaolinite particles (*i.e.,* the only suspended reagent that could be found in
375 this matrix). Ombaka [33] reported that kaolinite particles varied between 0.2 and 12 μm and Sun
376 et al. [17] found values ranging between 3.9 and 11.5 μm. According to Sun et al. [17], particle
377 size was proportional to turbidity. As in natural water, flocs formed in synthetic water presented
378 temporal evolution in size. Initial particles of up to 48 μm developed until reaching up to 265 μm
379 in diameter. As aggregation occurred, under different physical, chemical, and hydrodynamic
380 aspects, large, porous, branched, and irregular flocs were observed (Figure 4). Floc shape was
381 elliptical. The flocs did not obey *Euclidean* Geometry, in which, there is a uniform distribution
382 of mass on aggregates [28].
383 In the first images (Figure 4), it is possible to notice clusters of continuous evolution
384 during flocculation, with diameters ranging from 48 μm to 265 μm. Similar to what was
385 observed in the analysis of floc development in natural water, the concentration of primary
386 particles in the medium decreased due to the formation of aggregates. However, the synthetic
387 matrix showed high turbidity due to the presence of kaolinite to the medium. Besides, at the end
388 of the treatment, the precipitates were possibly constituted by the amorphous form of the

chemical coagulants, such as aluminium hydroxide, with kaolinite particles being randomly distributed by their structure. The same statement cannot be applied to flocs formed using natural coagulants or treatment of natural water, since the heterogeneous composition requires specific analyses and methodologies. Just as Yu et al. [26] reported the dependence of floc properties related to the type of coagulant, the acquired images illustrated that coagulation and mixing conditions, coagulation mechanisms, and water matrix characteristics also influenced the development of the flocs.

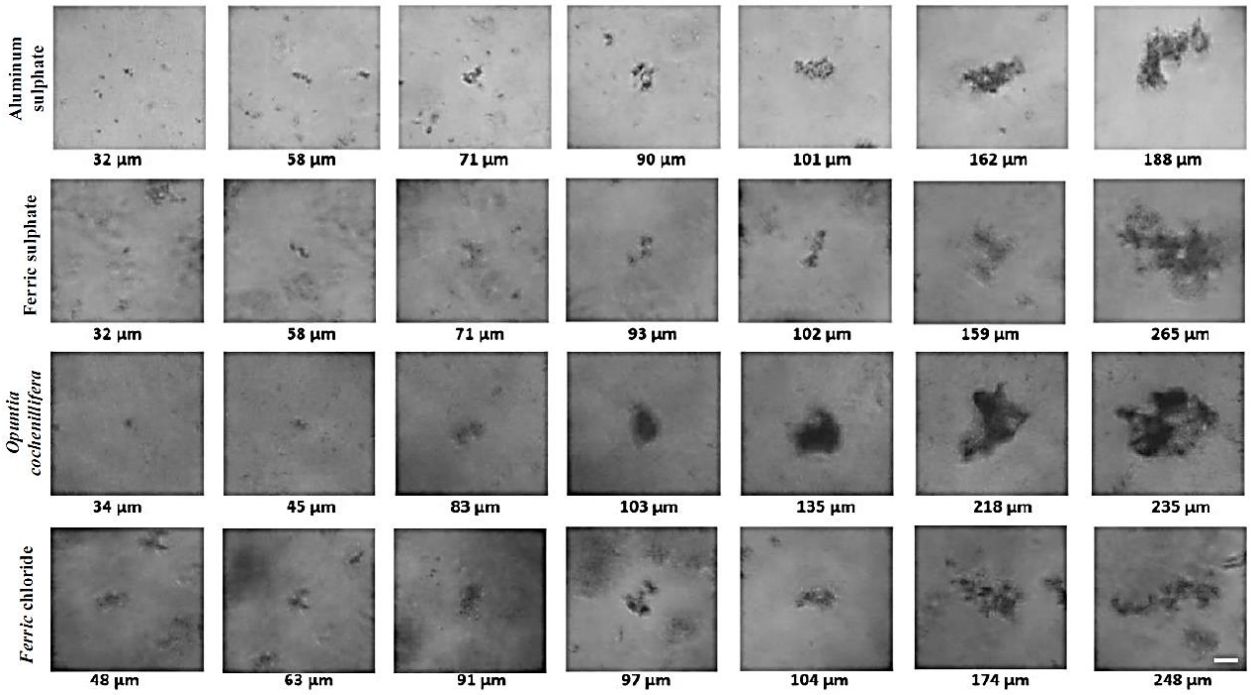

Figure 4. Examples of *in-situ* floc images captured during the synthetic water flocculation process using different coagulants. Non-corresponding floc portraits are shown. The portraits were cropped from original images (1392 × 1040 pixels) by the algorithm. The values indicate the Feret's diameter. Difference in sharpness refers to turbidity and the water matrix under study (Scale bar = 50 µm).

403 The relative frequency of flocs of different diameters for each coagulant tested treating
404 synthetic water was also determined (Figure 5). Although flocs reached larger diameters in the
405 synthetic matrix, 90% of the diameter values were between 20 and 200 μm. Among the
406 coagulants, ferric chloride and ferric sulphate resulted in a larger concentration of flocs with
407 diameters between 41 and 50 μm, and aluminium sulphate and *O. cochenillifera* between 31 and
408 40 μm. Because it presented larger turbidity and, consequently, more dispersed particles within, a
409 larger particle size distribution was expected for this test water. This was confirmed by the
410 variation in the floc diameters (19 - 21607 μm, Table S3) in our assays. This larger interval is the
411 result of larger numbers of collisions between particles, between particles and clusters, and
412 between clusters [34]. These flocs are expected to be more compact than those formed by natural
413 water due to the number of collisions. Compact flocs have higher sedimentation velocities
414 compared to more porous flocs with the same volume and constitution [12].

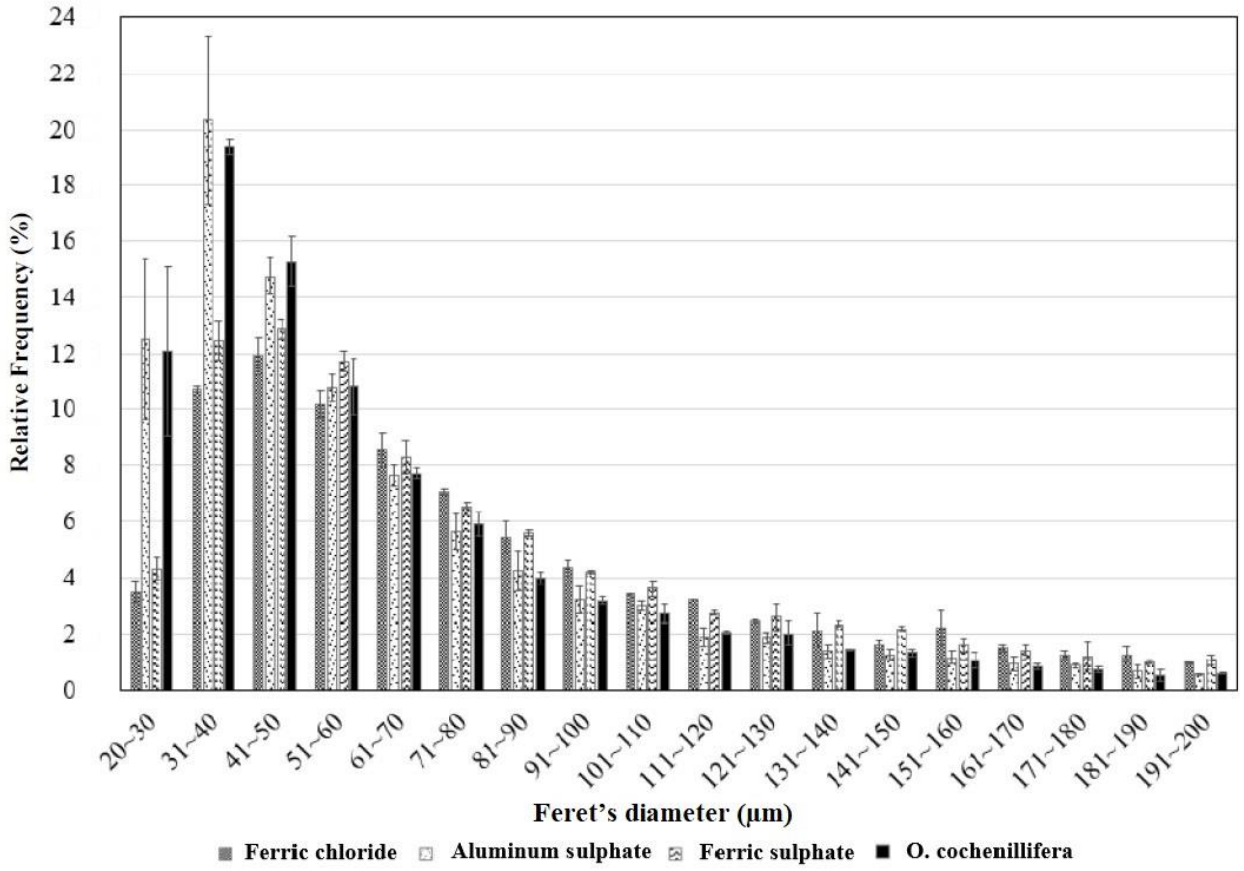

Figure 5. Relative frequency of flocs (Feret's diameter range) formed during flocculation of the synthetic water. The results were obtained by evaluating 500 images for each coagulant.

Resembling the assays with natural water, ferric coagulants resulted in flocs up to 2-fold larger than those formed by aluminium sulphate; this same behaviour was observed by Turchiuli and Fargues [15], who compared ferric and aluminium-based coagulants. Flocs formed using ferric chloride and ferric sulphate showed an average diameter of 170 μm and 145 μm, respectively. Besides, it was expected that *O. cochenillifera* would lead to larger flocs, but differently from the assays using the natural water matrix, the natural coagulant on synthetic water pointed to a larger variation and heterogeneity of floc size. However, the average floc diameter using natural coagulant was the smallest among the coagulants treating synthetic water.

Differences in the average size of flocs and number of flocs were observed when analysing the generated peaks (Figure S2). During the initial 2.5 minutes of the aluminium sulphate assays, we observed that the number of flocs declined. Meanwhile, despite the curve indicating rupture of the flocs at the end, we noted significant evolution in the average size of the flocs over time, making the synthetic water clarified. Regarding ferric sulphate, a decrease in number of particles was also observed, however, this behaviour might not have been caused by the formation of larger aggregates. As the application of ferric sulphate provided removal of turbidity and apparent colour larger than 99 and 88%, respectively, it was observed that, in less than 5 minutes of flocculation, the imaged flocs reached sizes much larger than the field of view of the imaging system. To avoid inaccurate measurements, they were discarded by the algorithm from further analysis.

By analysing the evolution of flocs in assays using ferric chloride, we noticed that floc size increased in almost 6-fold the initial average value, exhibiting a diameter of 473 μm. This constant increase in size was accompanied by a decrease of approximately half of the average number of flocs from the liquid medium. This pattern is consistent with the high and satisfactory removal performance of colour and turbidity obtained. Previously, in assays using *O. cochenillifera*, inconsistencies such as irregular growth and decrease trends were observed, which made it difficult to interpret the relationships between the increasing aggregate size and the water clarifying process [9].

4. Conclusion

The *in-situ* microscopy technique allowed obtaining images of the initial development of flocs, as well as to determine their size distributions, and to evaluate their formation and

450 breaking along the flocculation process. Through the captured images, we observed
451 heterogeneity of flocs' size and shape. Size distribution was found to be wider in synthetic water
452 (19 - 21607 μm) than in natural water (19 - 15834 μm), favouring the occurrence of shocks and
453 collisions in the medium, which were responsible for floc formation and development. When
454 comparing the two water matrices, these results showed the influence of the initial concentration
455 of particles on floc development. With a higher concentration of particles in the matrix, due to
456 the addition of kaolinite, observed aggregates in synthetic water for all coagulants were higher
457 than those obtained in natural water.

458 Overall, our results assisted elucidating the complexity of evaluating floc formation in
459 different water systems. Distinct types of coagulants, mixing conditions, use of alkalinizers,
460 presence or absence of organic matter, test durations, among other factors must be analysed in
461 detail, to complement the results obtained from this study. Due to the use of a fixed optical
462 magnification, the *in-situ* microscopy did not allow us to evaluate floc development along the
463 complete flocculation process, demonstrating some limitations of the technique in the present
464 conditions. It should also be noted that the success of the coagulation treatment, as well as floc
465 development, do not depend on isolated factors, such as dosage and pH. Other aspects involve
466 mixing conditions, the formation (and general characteristics) of sludge, breaking and regrouping
467 of flocs, and resistance, for example, also interfere on the efficiency of the water treatment. This
468 invites further research to better elucidate in-situ microscopy for floc development and/or water
469 treatment monitoring, including said factors, as well as challenging contaminants and other
470 coagulants, both conventional and new.

471

472

Acknowledgements

This work was supported by the Global Challenges Research Fund (GCRF) UK Research and Innovation (SAFEWATER; EPSRC Grant Reference EP/P032427/1), and The National Council for Scientific and Technological Development (CNPq - Brazil) for the MSc scholarship awarded to Gustavo Santos Nunes.

Authors' contribution

G. S. N.: Conceptualization, methodology - laboratory experiments, formal analysis, investigation, data curation, writing - original draft, review & editing, visualization; **K. J. S. S.:** Writing - review & editing; **B. L. S. F.:** Writing - review & editing; **V. L. B.:** Conceptualization, methodology - software, formal analysis, investigation, resources, data curation, writing - review & editing; **L. P. S. P.:** Conceptualization, resources, writing - review & editing, supervision, project administration, funding acquisition.

Statement

Authors declare previous originality check, no conflict of interest and open access to the repository of data used in this research.

Supplementary Material

Details of water and floc characterization are provided as supplementary material.

References

[1] Kim, S.H., Moon, B.H., Lee, H.I., 2001. Effects of pH and dosage on pollutant removal and

floc structure during coagulation. Microchem. J. 68, 197–203. https://doi.org/10.1016/S0026-265X(00)00146-6

[2] Xiao, F., Simcik, M.F., Gulliver, J.S., 2013. Mechanisms for removal of perfluorooctane sulfonate (PFOS) and perfluorooctanoate (PFOA) from drinking water by conventional and enhanced coagulation. Water Res. 47(1), 49–56. https://doi.org/10.1016/j.watres.2012.09.024

[3] Mcconnachie, G.L., Folkard, G.K., Mtawalic, M.A., Sutherland, J.P., 1999. Field trials of appropriate hydraulic flocculation processes. Water Res. 33(6), 1425–1434. https://doi.org/10.1016/S0043-1354(98)00339-X

[4] Baghvand, A., Zand, A.D., Mehrdadi, N., Karbassi, A., 2010. Optimizing Coagulation Process for Low to High Turbidity Waters Using Aluminum and Iron Salts. Am. J. Environ. Sci. 6(5), 442–448. https://doi.org/10.3844/ajessp.2010.442.448

[5] Chakraborti, R.K., Gardner, K.H., Atkinson, J.F., Van Benschoten, J.E., 2003. Changes in fractal dimension during aggregation. Water Res. 37, 873–883. https://doi.org/10.1016/S0043-1354(02)00379-2

[6] Chakraborti, R.K., Atkinson, J.F., Van Benschoten, J.E., 2000. Characterization of alum floc by image analysis. Environ. Sci. Technol. 34(18), 3969–3976. https://doi.org/10.1021/es990818o

[7] Mccurdy, K., Carlson, K., Gregory, D., 2004. Floc morphology and cyclic shearing recovery: Comparison of alum and polyaluminum chloride coagulants. Water Res. 38(2), 486–494. https://doi.org/10.1016/j.watres.2003.10.005

[8] Sillanpää, M., Ncibi, M.C., Matilainen, A., Vepsäläinen, M., 2018. Removal of natural organic matter in drinking water treatment by coagulation: A comprehensive review. Chemosphere, 190, 54–71. https://doi.org/10.1016/j.chemosphere.2017.09.113

519 [9] Shilpa, B.S., Akankshaa, Kavita, Girish, P., 2012. Evaluation of Cactus and Hyacinth Bean
520 Peels as Natural Coagulants. Int. J. Chem. Environ. Eng. 3(3).
521 https://doi.org/10.13140/RG.2.2.31066.98247
522 [10] Yin, C.Y., 2010. Emerging usage of plant-based coagulants for water and wastewater
523 treatment. Process Biochem. 45(9), 1437–1444. https://doi.org/10.1016/j.procbio.2010.05.030
524 [11] Oladoja, N.A., 2015. Headway on natural polymeric coagulants in water and wastewater
525 treatment operations. J. Water Process. Eng. 6, 174–192.
526 https://doi.org/10.1016/j.jwpe.2015.04.004
527 [12] Oliveira, A.L., Moreno, P., Silva, P.A.G., Julio, M., Moruzzi, R.B., 2016. Effects of the
528 fractal structure and size distribution of flocs on the removal of particulate matter. Desalin.
529 Water Treat. 57(36), 16721-16732. https://doi.org/10.1080/19443994.2015.1081833
530 [13] Lapointe, M., Barveau, B., 2016. Characterization of ballasted flocs in water treatment using
531 microscopy. Water Res. 90, 119–127. https://doi.org/10.1016/j.watres.2015.12.018
532 [14] Vlieghe, M., Frances, C., Coufort-Saudejaud, C., Liné A., 2017. Morphological Properties
533 of Flocs Under Turbulent Break-Up and Restructuring Processes. AIChE J., 63(9).
534 https://doi.org/10.1002/aic.15745
535 [15] Turchiuli, C., Fargues, C., 2004. Influence of structural properties of alum and ferric flocs
536 on sludge dewaterability. Chem. Eng. J. 103, 1-3, 123–131.
537 https://doi.org/10.1016/j.cej.2004.05.013
538 [16] Jarvis, P., Jefferson, B., Parsons, S.A., 2005. How the Natural Organic Matter to Coagulant
539 Ratio Impacts on Floc Structural Properties. Environ. Sci. Technol. 39(22), 8919-8924.
540 https://doi.org/10.1021/es0510616
541 [17] Sun, S., Weber-Shirk, M., Lion, L.W., 2016. Characterization of Flocs and Floc Size

542 Distributions Using Image Analysis. Environ. Eng. Sci. 33(1), 25–34.
543 https://doi.org/10.1089/ees.2015.0311
544 [18] Maciver, M.R., Pawlik, M., 2017. Analysis of In Situ Microscopy Images of Flocculated
545 Sediment Volumes. Chem Eng Technol. 40(12), 2305–2313.
546 https://doi.org/10.1002/ceat.201600523
547 [19] Miller, S.M., Fugate, E.J., Craver, V.O., Smith, J.A., Zimmerman, J.B., 2008. Toward
548 Understanding the Efficacy and Mechanism of Opuntia spp. as a Natural Coagulant for
549 Potential Application in Water Treatment. Environ. Sci. Technol. 42(12). https://doi.org/
550 10.1021/es7025054
551 [20] American Public Health Association – APHA, American Water Works Association –
552 AWWA, World Economic Forum – WEF. 2012. Standard Methods for the Examination of
553 Water and Wastewater. New York: American Public Health Association.
554 [21] Di Bernardo, L., Dantas, A.D.B., Voltan, P.E.N., 2011. Treatability of Water and
555 Wastewater Generated in Water Treatment Plants [Tratabilidade de Água e dos Resíduos
556 Gerados em Estações de Tratamento de Água]. Editora LDiBe.
557 [22] Souza Freitas, B.L., Sabogal-Paz, L.P., 2020. Pretreatment using Opuntia cochenillifera
558 followed by household slow sand filters: technological alternatives for supplying isolated
559 communities. Environ. Technol. 41(21):2783-2794. https://doi.org/
560 10.1080/09593330.2019.1582700
561 [23] Suhr, H., Wehnert, G., Schneider, K., Bittner, C., Scholz, T., Geissler, P., Jähne, B.,
562 Scheper, T. 1995. In situ microscopy for on-line characterization of cell-populations in
563 bioreactors, including cell-concentration measurements by depth from focus. Biotechnol.
564 Bioeng. 47, 106-116. https://doi.org/ 10.1002/bit.260470113

565 [24] Wiedemann, P., Guez, J.S., Wiegemann, H.B., Egner, F., Quintana, J.C., Asanza-
566 Maldonado, D., Filipaki, M., Wilkesman, J., Schwiebert, C., Cassar, J.P., Dhulster, P., Suhr,
567 H. 2011. In situ microscopic cytometry enables noninvasive viability assessment of animal
568 cells by measuring entropy states. Biotechnol. Bioeng. 108, 2884-2893. https://doi.org/
569 10.1002/bit.23252
570 [25] Gonzalez, R., Woods, R. Digital image processing. 3rd Ed. Pearson Education, 2008.
571 [26] Yu, J., Wang D., Yan M., Ye C., Yan M., Ge X., 2007. Optimized coagulation of high
572 alkalinity, low temperature and particle water: pH adjustment and polyelectrolytes as
573 coagulant aids. Environmental Monitoring and Assessment. 131, 377-386.
574 https://doi.org/10.1007/s10661-006-9483-3
575 [27] Yang, Z., Gao, B., Yue Q., 2010. Coagulation performance and residual aluminium
576 speciation of $Al_2(SO_4)_3$ and polyaluminium chloride (PAC) in Yellow River water treatment.
577 Chemical Engineering Journal. 165(1), 122-132. https://doi.org/10.1016/j.cej.2010.08.076
578 [28] Chakraborti, R.K., Gardner, K.H., Kaur, J., Atkinson, J.F., 2007. In situ analysis of flocs. J.
579 Water Supply Res. T. 56 (1): 1–11. https://doi.org/10.2166/aqua.2007.063
580 [29] Jiao, R., Fabris, R., Chow, C.W.K., Drikas, M., Leeuwen, J., Wang, D., Xu, Z. 2017.
581 Influence of coagulation mechanisms and floc formation on filterability. J. Environ. Sci. 57,
582 338–345. https://doi.org/10.1016/j.jes.2017.01.006
583 [30] Duan, J., Gregory, J., 2003. Coagulation by hydrolysing metal salts. Adv. Colloid Interface
584 Sci. (100-102), 475-502. https://doi.org/10.1016/S0001-8686(02)00067-2
585 [31] Jarvis, P., Sharp, E., Pidou, M., Molinder, R., Parsons, S.A., Jefferson, B. 2012. Comparison
586 of coagulation performance and floc properties using a novel zirconium coagulant against
587 traditional ferric and alum coagulants. Water Res. 46(13), 4179–4187.

https://doi.org/10.1016/j.watres.2012.04.043

[32] Moruzzi, R.B., Silva, P.G., Sharifi, S., Campos, L.C., Gregory, J. 2019. Separation and Purification Technology Strength assessment of Al-Humic and Al-Kaolin aggregates by intrusive and non-intrusive methods. Sep. Purif. Technol. 217, 265–273. https://doi.org/10.1016/j.seppur.2019.02.033

[33] Ombaka, O., 2016. Characterization and classification of clay minerals for potential applications in Rugi Ward, Kenya. African Journal of Environmental Science and Technology. 10(11), 415-431. https://doi.org/10.5897/AJEST2016.2184

[34] Hopkins, D.C., Ducoste, J.J., 2003. Characterizing flocculation under heterogeneous turbulence. J. Colloid Interface Sci. 264(1), 184–194. https://doi.org/10.1016/S0021-9797(03)00446-6

Supplementary material

In-situ microscopy investigation of floc development during coagulation-flocculation with chemical and natural coagulants

Gustavo Santos Nunes[a], Kamila Jessie Sammarro Silva[a]; Bárbara Luíza Souza Freitas[a;] Valdinei Luís Belini[b]; Lyda Patricia Sabogal-Paz[a*]

[a] Department of Hydraulic and Sanitation, São Carlos School of Engineering, University of São Paulo, Trabalhador São-Carlense Avenue 400, São Carlos, São Paulo, 13566-590, Brazil

[b.] Department of Electrical Engineering, Federal University of São Carlos, Rodovia Washington Luís, km 235. São Carlos, São Paulo, 13566-905, Brazil.

* Corresponding Author: lysaboga@sc.usp.br

	Natural water				Synthetic water			
Coagulant*	AS	FS	FC	OC	AS	FS	FC	OC
Temperature (°C)	23	22	21	21	21	21	24	23
Turbidity (NTU)	0.26 ± 0.05**	0.26 ± 0.03	0.17 ± 0.01	5.67 ± 0.18	0.60 ± 0.02	0.71 ± 0.02	0.66 ± 0.16	3.17 ± 0.42
Apparent colour (uH)	3.20 ± 0.69	5.53 ± 2.16	2.93 ± 0.75	25.83 ± 2.57	3.63 ± 0.06	7.17 ± 1.25	11.27 ± 0.35	32.93 ± 0.83
True colour (uH)	1.40 ± 0.60	0.00 ± 0.00	0.00 ± 0.00	8.53 ± 0.25	0.67 ± 0.15	0.13 ± 0.23	4.97 ± 0.46	23.50 ± 0.72
Electric conductivity (μS cm^{-2})	86.55 ± 1.07	94.48 ± 1.36	67.15 ± 0.62	107.92 ± 1.09	77.35 ± 1.03	100.64 ± 1.36	68.94 ± 0.84	156.60 ± 63.53
Partial alkalinity (mg $CaCO_3\,L^{-1}$)	8.44 ± 0.27	14.79 ± 0.67	4.99 ± 0.31	36.98 ± 0.77	12.03 ± 0.96	9.35 ± 0.57	8.02 ± 0.71	63.53 ± 2.15
Total alkalinity (mg $CaCO_3\,L^{-1}$)	12.12 ± 0.67	20.14 ± 0.86	9.00 ± 0.31	44.02 ± 1.11	6.5 ± 0.56	2.74 ± 0.43	3.56 ± 0.16	73.24 ± 1.93
Zeta potential (mV)	-19.40 ± 4.25	-23.53 ± 4.03	-16.17 ± 2.42	-29.57 ± 3.86	-18.43 ± 6.99	-11.87 ± 10.38	-17.19 ± 7.99	-30.26 ± 2.12
DOC (mg L^{-1})	2.96 ± 0.20	2.52 ± 0.20	1.25 ± 0.82	5.59 ± 0.28	1.60 ± 0.06	1.28 ± 0.21	1.90 ± 0.05	2.96 ± 0.20

Table S1. Physicochemical characterization** of clarified water after performing jar test assays

(*) AS = Aluminium sulphate; FS = Ferric sulphate; FC = Ferric chloride; OC = *Opuntia cochenillifera*; DOC = dissolved organic carbon.

(**) The results are presented as M ± SD. where M = mean; SD = standard deviation

618

619

Coagulant	Mean Feret's Diameter (µm)	Standard deviation (µm)	Median (µm)	Minimum value (µm)	Maximum value (µm)
Ferric chloride	108.05	2.13	60	21	10839
Aluminium sulphate	101.26	11.78	52	19	4806
Ferric sulphate	108.44	3.26	59	21	15834
Opuntia sp.	126.85	9.82	69	20	8643

620 Table S2. Characteristics of aggregates formed in natural water using in-situ imaging technique.

621

Coagulant	Mean Feret's Diameter (µm)	Standard deviation (µm)	Median (µm)	Minimum value (µm)	Maximum value (µm)
Ferric chloride	169.63	2.48	78	20	20524
Aluminium sulphate	86.70	15.20	53	19	7195
Ferric sulphate	144.96	5.12	71	21	19967
Opuntia sp.	96.64	15.41	54	21	21607

Table S3. Characteristics of aggregates formed in natural water using *in-situ* imaging technique.

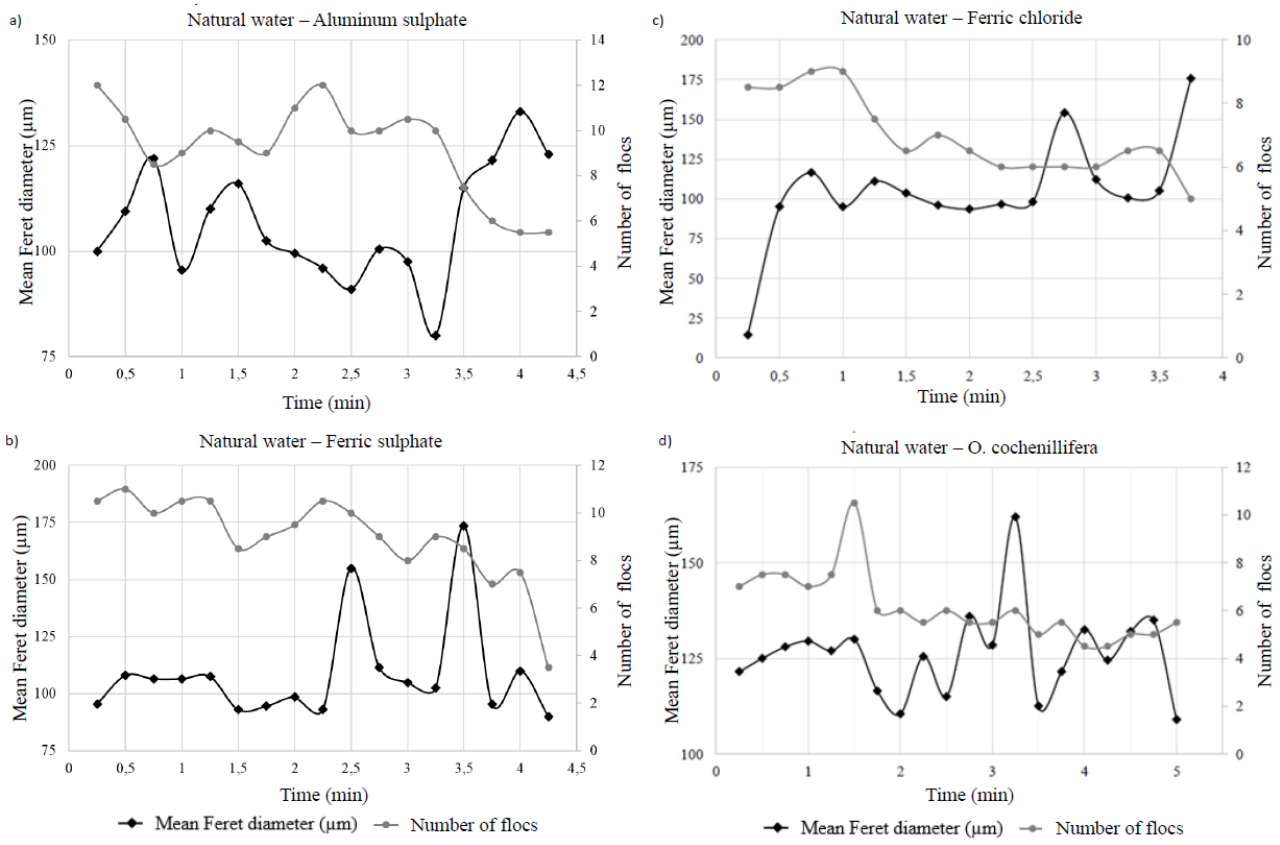

636

637 Figure S1. Floc growth in natural water. a) aluminium sulphate; b) ferric sulphate; c) ferric

638 chloride; d) *Opuntia* sp.

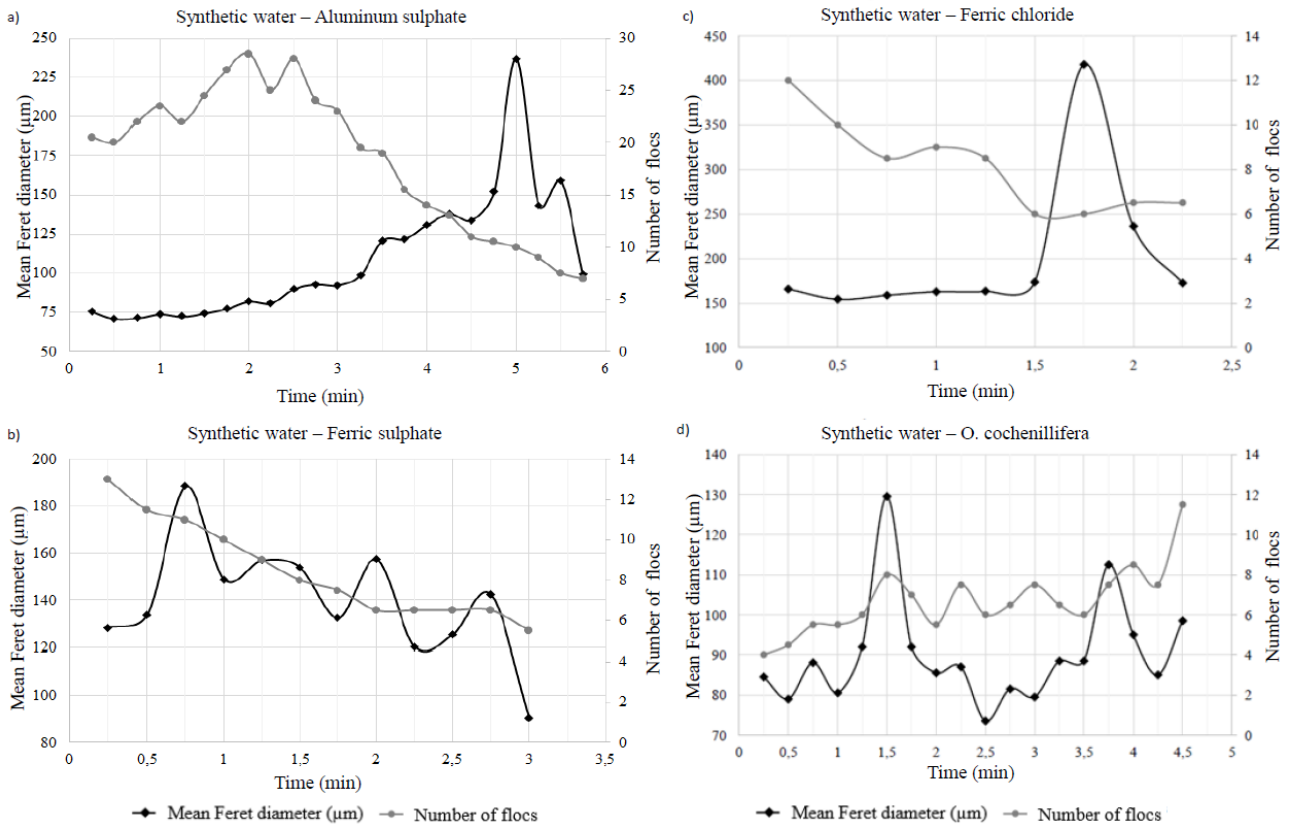

Figure S2. Floc growth in synthetic water. a) aluminium sulphate; b) ferric sulphate; c) ferric chloride; d) *Opuntia* sp.